Model for the reversible magnetization of high-κ type-II superconductors: Application to high-T_c superconductors

Zhidong Hao and John R. Clem
Ames Laboratory–U.S. Department of Energy and Department of Physics, Iowa State University, Ames, Iowa 50011

M. W. McElfresh, L. Civale, A. P. Malozemoff, and F. Holtzberg
IBM Thomas J. Watson Research Center, Yorktown Heights, New York 10598-0218

(Received 12 June 1990)

A simple theoretical model is proposed for the reversible magnetization of type-II superconductors as a function of the applied field H for the entire field region between H_{c1} and H_{c2}. For $H \simeq H_{c1}$, the theory reduces to a variational model, from which H_{c1} can be accurately computed in the Ginzburg-Landau regime. In calculating the free energy, we include, in addition to the supercurrent kinetic energy and the magnetic-field energy, the kinetic-energy and the condensation-energy terms arising from suppression of the order parameter in the vortex core. The model is further extended to include anisotropy by introducing an effective-mass tensor for the case when H is parallel to one of the principal axes. The theory is compared to reversible-magnetization data on a $YBa_2Cu_3O_7$ single crystal. The method permits an accurate determination of H_{c2} versus temperature from measurements of the magnetization versus temperature at fixed magnetic field and explains why the measurements have different slopes in different fields, contrary to what might have been expected from the linear Abrikosov formula near H_{c2}. The deduced dH_{c2}/dT is (-1.65 ± 0.23) T/K for H parallel to the c axis near T_c, implying $\xi_{ab}(0)=(17\pm1)$ Å.

I. INTRODUCTION

The vortex structure of a type-II superconductor was first studied by Abrikosov,[1] based on the Ginzburg-Landau equations,[2] for the cases of low and high magnetic field H, i.e., $H-H_{c1} \ll H_{c1}$ and $H_{c2}-H \ll H_{c2}$, where H_{c1} and H_{c2} are the lower and upper critical fields, respectively. For the intermediate field $H_{c1} \ll H \ll H_{c2}$, where the Ginzburg-Landau equations cannot be solved in closed form due to their nonlinearity, the London model[3,4] has provided the only detailed phenomenological description for extreme type-II superconductors for which the Ginzburg-Landau parameter $\kappa=\lambda/\xi$ obeys $\kappa \gg 1$ (here λ is the penetration depth and ξ is the coherence length). In the London model the local magnetic flux density of a type-II superconductor in the mixed state (vortex state) is represented by a linear superposition of the fields of isolated vortices, which is valid only when κ is large and the vortex spacing is large compared with ξ. Although the London model can give a good qualitative account of the mixed state in the restricted field region, it suffers from its singular property that both the magnetic flux density and the supercurrent density of an isolated vortex diverge on the axis of the vortex, because the depression of the order parameter to zero on the axis is not accounted for by the model.

In Ref. 5, one of the authors proposed a variational model for an isolated vortex, which reduces to the London model outside the vortex core but has the added advantage of yielding realistic results in the vortex core vicinity. Simple analytic expressions for the magnetic flux density and supercurrent density of an isolated vortex easily can be obtained from this model, and they have the same qualitative behavior as found by solving the Ginzburg-Landau equations numerically. In Ref. 6, it is argued that the procedure of obtaining the local magnetic flux density by a linear superposition of contributions of individual vortices is valid for arbitrary κ and vortex spacing, provided these contributions are calculated using the correct spatially-dependent magnitude of the order parameter that is appropriate for the given vortex spacing.

In this paper we extend the work of Refs. 5 and 6 to construct a model for the mixed state of a type-II superconductor and compare it to experimental results on a $YBa_2Cu_3O_7$ single crystal. This test case is of particular significance because of the considerable ambiguity in the determination of H_{c2} of the high-temperature superconductors.[7] Here we will focus on a "diamagnetic H_{c2}," the upper critical field for the onset of diamagnetism (in a mean-field sense, ignoring diamagnetic fluctuations at higher temperatures). It is now widely recognized that the magnetic phase diagram of these superconductors contains a vortex fluid regime at the temperatures just below the diamagnetic H_{c2}, in which the magnetization behavior is fully reversible and the transport data show flux flow. According to Fisher, Fisher, and Huse,[8] because the phase γ of the local superconducting order parameter Ψ varies with the Brownian motion of the vortices, a nonzero voltage appears for arbitrarily small applied currents, and so, strictly speaking, this regime is not superconducting, even though it may show substantial diamagnetism. This suggests that the diamagnetic H_{c2} is only a crossover, rather than a true phase transition as in

the usual mean-field theory.

Nevertheless we presume that entropic effects in this regime are small, so that the diamagnetism of the vortex fluid resembles closely that of an ideal Abrikosov mixed state. Indeed, our theoretical treatment also neglects the specifically hexagonal vortex structure and merely assumes some averaged close-packed configuration.

The mixed-state diamagnetism can readily be measured, and, when compared to theory, can give the diamagnetic H_{c2}. Close enough to H_{c2}, the diamagnetism is given by[1]

$$-4\pi M=\frac{H_{c2}(T)-H}{(2\kappa^2-1)\beta_A} , \tag{1}$$

where β_A is 1.16 for a hexagonal array. This suggests that a linear extrapolation of $M(H)$ or $M(T)$ data should determine $H_{c2}(T)$. Welp *et al.*[9] first carried out such experiments on a $YBa_2Cu_3O_7$ crystal and deduced in this way a linear dependence of H_{c2} on temperature, with slopes of -1.9 T/K and -10 T/K for a field parallel to the c and the ab axes, respectively. As we shall show, our data are substantially the same as those of Welp *et al.*

Nevertheless, their data for $M(T)$, and ours, show a noticeable field dependence in the slope dM/dT, in contrast to the prediction of Eq. (1). This leads to the peculiar result that if the same data are plotted as $M(H)$ at fixed temperatures and extrapolated to determine $H_{c2}(T)$, the $H_{c2}(T)$ is *nonlinear* with, on average, much lower slopes than those quoted above. Therefore there is a serious ambiguity in determining the correct $H_{c2}(T)$, which the theory in this paper can help resolve. As we shall see, much of the data correspond to fields H far below $H_{c2}(T)$ and thus are not adequately described by Eq. (1). The more complete theoretical treatment explains the field-dependent dM/dT slopes and restores the linear $H_{c2}(T)$ behavior, but leads to a somewhat revised value of -1.65 T/K for dH_{c2}/dT with the field parallel to the c axis.

Another issue addressed by the experimental results is whether $YBa_2Cu_3O_7$ falls in the clean or dirty superconducting limit. Our crystals show resistivities in the range 50–80 $\mu\Omega$ cm just above T_c,[10] whereas the crystal of Welp *et al.* shows 120 $\mu\Omega$ cm. In the dirty limit, dH_{c2}/dT should scale linearly with resistivity. The similarity of our results and those of Welp *et al.* confirms the clean-limit behavior of these materials parallel to the CuO_2 planes, which has also been deduced from transport[11] and optical[12] measurements.

In Sec. II we give the details of our model and obtain an expression for the reversible magnetization of an isotropic type-II superconductor. In Sec. III we take the effect of anisotropy into account. In Sec. IV we report experimental results on a $YBa_2Cu_3O_7$ single crystal, compare the results to the theory, and summarize.

II. REVERSIBLE MAGNETIZATION OF TYPE-II SUPERCONDUCTORS

We consider an infinite type-II superconductor in the mixed state. As can be shown,[2,4,13] the Ginzburg-Landau free energy per unit volume over cross-sectional area A in a plane perpendicular to the vortices, measured relative to that of the Meissner state, can be expressed in dimensionless form as

$$F=F_c+F_{kg}+F_{kj}+F_f , \tag{2}$$

where

$$F_c=\frac{1}{A}\int d^2\rho\tfrac{1}{2}(1-f^2)^2 , \tag{3}$$

$$F_{kg}=\frac{1}{A}\int d^2\rho\frac{1}{\kappa^2}(\nabla f)^2 , \tag{4}$$

$$F_{kj}=\frac{1}{A}\int d^2\rho f^2\mathbf{a}_s^2 \quad \left[\mathbf{a}_s=\mathbf{a}+\frac{1}{\kappa}\nabla\gamma\right] , \tag{5}$$

and

$$F_f=\frac{1}{A}\int d^2\rho\,\mathbf{b}^2 \tag{6}$$

are the *condensation* energy, *kinetic* energy associated with *gradients* in the magnitude of order parameter, *kinetic* energy associated with *supercurrent,* and *magnetic field* energy; f and γ are the normalized magnitude and phase of the order parameter $\Psi=\Psi_0 f e^{i\gamma}$ (Ψ_0 is the magnitude of order parameter in absence of field); $\mathbf{a}$ is the vector potential satisfying $\nabla\cdot\mathbf{a}=0$; $\mathbf{b}=\nabla\times\mathbf{a}$ is the local magnetic flux density; and the two-dimensional integral is taken over A.

We use in this paper dimensionless units, which correspond to measuring the magnitude of the order parameter in units of Ψ_0, length in units of λ, magnetic field in units of $\sqrt{2}H_c=\kappa\phi_0/2\pi\lambda^2$, vector potential in units of $\sqrt{2}H_c\lambda=\kappa\phi_0/2\pi\lambda$, and energy in units of $H_c^2/4\pi$, where H_c is the thermodynamic critical field, and $\phi_0=hc/2e=2.07\times10^{-7}$ G cm^2 is the flux quantum (ϕ_0 corresponds to $2\pi/\kappa$ in the dimensionless expressions).

In Ginzburg-Landau theory, the temperature dependence of a superconductor is contained in the scaling factors, such as $\sqrt{2}H_c(T)$ and $\lambda(T)$, and therefore all physical quantities in their dimensionless form are independent of T, and the only parameter intrinsic to the sample is κ.

The second Ginzburg-Landau equation is

$$\mathbf{j}=-f^2\mathbf{a}_s , \tag{7}$$

where $\mathbf{j}$ is the supercurrent density.

For a vortex centered on the z axis, in terms of cylindrical coordinates ρ, ϕ, and z, with unit vectors $\hat{\boldsymbol{\rho}}$, $\hat{\boldsymbol{\phi}}$, and $\hat{\mathbf{z}}$, $\gamma=-\phi$, $\mathbf{b}=\hat{\mathbf{z}}b_z(\rho)$, $\mathbf{j}=\hat{\boldsymbol{\phi}}j_\phi(\rho)$, and $\mathbf{a}=\hat{\boldsymbol{\phi}}a_\phi(\rho)$. We have $\nabla\gamma=-\nabla\phi=-\hat{\boldsymbol{\phi}}(1/\rho)$, $\mathbf{a}_s=\hat{\boldsymbol{\phi}}(a_\phi-1/\kappa\rho)$, and therefore

$$\nabla\times\mathbf{a}_s=\hat{\mathbf{z}}\left[b_z-\frac{2\pi}{\kappa}\delta(\boldsymbol{\rho})\right] . \tag{8}$$

For an array of vortices at positions $\boldsymbol{\rho}_i$, we have

$$\nabla\times\mathbf{a}_s=\hat{\mathbf{z}}\left[b_z-\frac{2\pi}{\kappa}\sum_i\delta(\boldsymbol{\rho}-\boldsymbol{\rho}_i)\right] , \tag{9}$$

where each term in the summation represents one vortex carrying one quantum of magnetic flux centered at $\boldsymbol{\rho}_i$.

Using Eqs. (7) and (9), and with the help of Ampère's law $\mathbf{j}=\nabla\times\mathbf{b}$ and the divergence theorem, we find that the electromagnetic free energy per unit volume $F_{\rm em}=F_{kj}+F_j$ can be simply written as

$$F_{\rm em}=Bb_z(0)\ , \tag{10}$$

where $B=2\pi/\kappa A_{\rm cell}$ is the averaged magnetic flux density, $A_{\rm cell}$ is the unit-cell area of the flux-line lattice ($B=\phi_0/A_{\rm cell}$ in conventional units), and $b_z(0)$ is the local magnetic flux density at the center of a vortex resulting not only from the vortex's own field but also that of all surrounding vortices.

Our approach is to apply superposition and write

$$b_z(\boldsymbol{\rho})=\sum_i b_{0z}(\boldsymbol{\rho}-\boldsymbol{\rho}_i)\ , \tag{11}$$

where $b_{0z}(\boldsymbol{\rho}-\boldsymbol{\rho}_i)$ is the magnetic flux density of an isolated vortex located at $\boldsymbol{\rho}_i$, and the summation runs over all vortices; and to obtain b_{0z} we follow the procedure of Ref. 5 and take into account the effect of overlapping of vortices. We assume for the order parameter a trial function

$$f=\frac{\rho}{(\rho^2+\xi_v^2)^{1/2}}f_\infty\ , \tag{12}$$

where ξ_v and f_∞ are two variational parameters representing the effective core radius of a vortex and the depression in the order parameter due to overlapping of vortices, respectively. It is expected that $f_\infty\to 1$ as $B\to 0$ and $f_\infty\to 0$ as $B\to B_{c2}$ ($B_{c2}=H_{c2}=\kappa$ in the dimensionless units). Then, with the help of Ampère's law and $\mathbf{b}=\nabla\times\mathbf{a}$, the second Ginzburg-Landau equation can be solved analytically, and we find

$$b_{0z}=\frac{f_\infty K_0(f_\infty(\rho^2+\xi_v^2)^{1/2})}{\kappa\xi_v K_1(f_\infty\xi_v)}\ , \tag{13}$$

where $K_n(x)$ is a modified Bessel function of nth order.

We calculate b_z in the Appendix, where we introduce a Fourier transform of b_{0z}, transform the lattice summation in Eq. (11) into one in the corresponding reciprocal lattice, and then make the approximation of replacing the summation by an integral. Therefore, Eq. (10) becomes

$$F_{\rm em}=B^2+\frac{Bf_\infty K_0(\xi_v(f_\infty^2+2B\kappa)^{1/2})}{\kappa\xi_v K_1(f_\infty\xi_v)}\ . \tag{14}$$

With f being given by Eq. (12), F_c and F_{kg} are calculated by taking the integral over one lattice cell, which is approximated by a circle centered at a vortex axis and having the same cell area. As mentioned in the Introduction, this approximation means that we neglect the energy differences between specific vortex structures (hexagonal, square, amorphous,...), which we expect to be only a few percent. We find

$$F_c=\tfrac{1}{2}(1-f_\infty^2)^2+\frac{B\kappa\xi_v^2 f_\infty^2}{2}\left[(1-f_\infty^2)\ln\left[\frac{2}{B\kappa\xi_v^2}+1\right]+\frac{f_\infty^2}{2+B\kappa\xi_v^2}\right]\ , \tag{15}$$

and

$$F_{kg}=\frac{Bf_\infty^2(1+B\kappa\xi_v^2)}{\kappa(2+B\kappa\xi_v^2)^2}\ . \tag{16}$$

Now the variationally-calculated total free-energy density F is the sum of F_c, F_{kg}, and $F_{\rm em}$, given by Eqs. (15), (16), and (14), where the variational parameters f_∞ and ξ_v satisfy

$$\frac{\partial F}{\partial f_\infty}=0 \tag{17}$$

and

$$\frac{\partial F}{\partial \xi_v}=0\ . \tag{18}$$

The thermodynamic magnetic field H is given by

$$H=\frac{1}{2}\frac{dF}{dB}=\frac{1}{2}\left[\frac{\partial F}{\partial B}\right]_{f_\infty,\xi_v}\ , \tag{19}$$

where the second line is obtained by using Eqs. (17) and (18). By a straightforward calculation we find

$$H=\frac{\kappa f_\infty^2\xi_v^2}{2}\left[\frac{1-f_\infty^2}{2}\ln\left[\frac{2}{B\kappa\xi_v^2}+1\right]-\frac{1-f_\infty^2}{2+B\kappa\xi_v^2}+\frac{f_\infty^2}{(2+B\kappa\xi_v^2)^2}\right]+\frac{f_\infty^2(2+3B\kappa\xi_v^2)}{2\kappa(2+B\kappa\xi_v^2)^3}$$
$$+B+\frac{f_\infty}{2\kappa\xi_v K_1(f_\infty\xi_v)}\left[K_0(\xi_v(f_\infty^2+2B\kappa)^{1/2})-\frac{B\kappa\xi_v K_1(\xi_v(f_\infty^2+2B\kappa)^{1/2})}{(f_\infty^2+2B\kappa)^{1/2}}\right]\ , \tag{20}$$

where the first two terms correspond to F_c and F_{kg}, respectively, and the last two terms correspond to $F_{\rm em}$. The magnetization M is related to H by

$$-4\pi M=H-B\ . \tag{21}$$

Equations (20) and (21) give us the implicit function $M(H)$.

Note that H is the internal field, which is equal to the applied field only for a sample of zero demagnetization coefficient, but is approximately equal to the applied field when the demagnetization effect can be neglected. For the case when the demagnetization effect is important, H is equal to the applied field minus the field of demagnetization (see Ref. 4).

H_{c1} is given by the limit of H as $B \to 0$. We get

$$H_{c1}=\frac{\kappa\xi_{v0}^2}{8}+\frac{1}{8\kappa}+\frac{K_0(\xi_{v0})}{2\kappa K_1(\xi_{v0})} , \tag{22}$$

where ξ_{v0} is the value of ξ_v at $B=0$, which minimizes the free energy of a single vortex and satisfies

$$\kappa\xi_{v0}=\sqrt{2}\left[1-\frac{K_0^2(\xi_{v0})}{K_1^2(\xi_{v0})}\right]^{1/2} . \tag{23}$$

For $\kappa \gg 1$, we see that $\kappa\xi_{v0}\approx\sqrt{2}$. Note that both Eqs. (22) and (23) have been obtained in Ref. 5, which are the limits of our Eqs. (20) and (18) as $B \to 0$, as expected.

In principle, f_∞ and ξ_v are found for arbitrary B and κ by solving Eqs. (17) and (18) simultaneously, but this procedure involves numerical analysis and is not convenient in practical use. Instead we approximate $f_\infty(\kappa,B)$ and $\xi_v(\kappa,B)$ by some suitable functions. We find the following formulas are good approximations for the cases of $\kappa > 10$:

$$f_\infty^2=1-\left[\frac{B}{\kappa}\right]^4 , \tag{24}$$

$$\left[\frac{\xi_v}{\xi_{v0}}\right]^2=\left[1-2\left[1-\frac{B}{\kappa}\right]^2\frac{B}{\kappa}\right]\left[1+\left[\frac{B}{\kappa}\right]^4\right] . \tag{25}$$

For smaller κ the above formulas need modification; for example, for $\kappa\approx 5$, ξ_v is better approximated by

$$\left[\frac{\xi_v}{\xi_{v0}}\right]^2=1+\left[\frac{B}{\kappa}\right]^4 , \tag{26}$$

with f_∞ remaining unchanged as given by Eq. (24).

Curves of $-4\pi M(H)$ for the cases of $\kappa=5$ and 50 are calculated by using the above formulas and shown in Figs. 1(a) and 1(b). Abrikosov's high-field results, Eq. (1) with $\beta_A=1.16$, for the same values of κ are also shown for comparison. As can be seen, our results satisfy the qualitative properties of type-II superconductors: the slope $d(-4\pi M)/dH$ is infinite at H_{c1}; in the high-field region we recover the Abrikosov result that $-4\pi M$ decreases linearly as H increases and vanishes at H_{c2}. Because of our use of the circular cell approximation in Eqs. (15) and (16), the magnitude of the limiting slope of $-4\pi M$ versus H obtained from Eqs. (20) and (21) is actually slightly less than that of the Abrikosov result [Eq. (1) with $\beta_A=1.16$ for a hexagonal array] very close to H_{c2}. Nevertheless, as seen from Figs. 1(a) and 1(b), our results are practically indistinguishable from the linear Abrikosov curve over the field range $0.4H_{c2}<H<H_{c2}$. Quantitatively, as shown by the comparison with Abrikosov's high-field result, our results appear to be a good approximation to the solution of the Ginzburg-Landau equations.

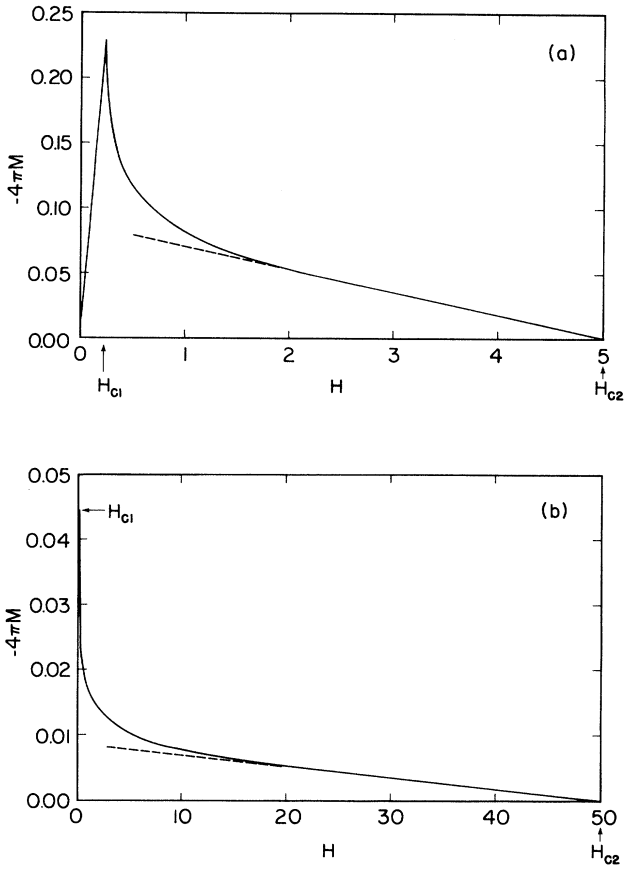

FIG. 1. Calculated $-4\pi M$ vs H in dimensionless units for (a) $\kappa=5$ and (b) $\kappa=50$, where the dashed lines are the corresponding Abrikosov high-field results.

III. EFFECTS OF ANISOTROPY ON THE MAGNETIZATION

In this section we generalize the model described in Sec. II to the case of anisotropic type-II superconductors. The anisotropy of superconductivity has been studied for a long time in the framework of Ginzburg-Landau theory by introducing a phenomenological effective-mass tensor M_{ij},[14-19] which has the principal values M_i $(i=1,2,3=a,b,c)$. The dimensionless units described in Sec. II remain unchanged if we take as the unit of length the scalar $\lambda=(\bar{M}c^2/16\pi e^2\Psi_0^2)^{1/2}$ with the mean mass $\bar{M}=(M_1M_2M_3)^{1/3}$, and express ξ and κ in terms of $\bar{M}$ by the usual relations $\xi=\phi_0/2\sqrt{2}\pi\lambda H_c$ and $\kappa=\lambda/\xi$. It is convenient to define a normalized mass tensor[18,19] $m_{ij}=M_{ij}/\bar{M}$ with principal values $m_i=M_i/\bar{M}$; then $m_1m_2m_3=1$.

If we choose a coordinate system aligned with the principal axes, then $m_{ij}=m_i\delta_{ij}$. In the anisotropic mass form the kinetic free-energy density terms are written as

$$F_{kg}=\frac{1}{A}\int d^2\rho\sum_i\frac{1}{\kappa^2 m_i}\left[\frac{\partial f}{\partial x_i}\right]^2 , \tag{27}$$

$$F_{kj}=\frac{1}{A}\int d^2\rho\sum_i\frac{f^2a_{si}^2}{m_i} . \tag{28}$$

Expressions for F_c and F_f remain the same as given by

Eqs. (3) and (6), since they do not involve mass explicitly (when written in conventional units). The second Ginzburg-Landau equation is

$$j_i = -\frac{f^2 a_{si}}{m_i} . \tag{29}$$

It was shown in Ref. 17 that the free-energy density and Ginzburg-Landau equations can be transformed to isotropic forms by a simple transformation if κ is replaced by a $\tilde{\kappa}$ that depends on the orientation of the vortices. This transformation was later shown to be valid only when H is along a principal axis.[18–20] We consider here only the case when H is applied along one of the principal axes. For vortices aligned along the x_3 axis, the transformation reads

$$\tilde{x}_i = \sqrt{m_3 m_i} x_i , \tag{30}$$

$$\tilde{b}_i = b_i \quad (b_i = b_3 \delta_{i3}) , \tag{31}$$

$$\tilde{a}_{si} = \frac{a_{si}}{\sqrt{m_i}} , \tag{32}$$

$$\tilde{j}_i = \sqrt{m_i} j_i , \tag{33}$$

and

$$\tilde{\kappa} = \frac{\kappa}{\sqrt{m_3}} . \tag{34}$$

This transformation preserves the relations that $\mathbf{j} = \nabla \times \mathbf{b}$, $\mathbf{b} = \nabla \times \mathbf{a}$, and $\nabla \cdot \mathbf{b} = 0$, and it suggests that we assume for the order parameter

$$f = \frac{\tilde{\rho}}{(\tilde{\rho}^2 + \xi_v^2)^{1/2}} f_\infty \tag{35}$$

with

$$\tilde{\rho}^2 = \frac{x_1^2}{m_2} + \frac{x_2^2}{m_1} , \tag{36}$$

which can be transformed to isotropic form [Eq. (12)] by the above transformation. Thus we can calculate the properties of the vortex state in the transformed frame exactly as in the isotropic case, except that the usual Ginzburg-Landau parameter κ is replaced by $\tilde{\kappa}$. Therefore, the final results can be obtained by simply replacing κ by $\tilde{\kappa}$ in the expressions for their isotropic counterparts. For example, for the isotropic case we have $H_{c2} = \kappa$ and $H = H(B, \kappa)$; then for the anisotropic case with the field applied along the x_3 axis we have $H_{c2} = \tilde{\kappa} = \kappa / \sqrt{m_3}$ and $H = H(B, \tilde{\kappa}) = H(B, \kappa / \sqrt{m_3})$, where $H(B, \kappa)$ is given by Eq. (20). Note that, if the vortices are aligned along the x_1 or x_2 axis, the corresponding results can be obtained by cyclic permutation ($1 \to 2 \to 3 \to 1$ or $a \to b \to c \to a$).

For the case that H is applied along arbitrary direction, H_{c2} has been found[15] by linearizing the first Ginzburg-Landau equation, i.e., essentially in the same fashion as in the isotropic case:

$$H_{c2} = \tilde{\kappa} , \tag{37}$$

where

$$\tilde{\kappa} = \frac{\kappa}{\alpha} , \tag{38}$$

$$\alpha = (m_1 \sin^2\theta \cos^2\phi + m_2 \sin^2\theta \sin^2\phi + m_3 \cos^2\theta)^{1/2} , \tag{39}$$

and θ and ϕ are the polar and azimuthal angles of the applied field with respect to the principal axes. Equation (34), for example, corresponds to the case when $\theta = 0$. For lower fields, when the field is not applied along one of the principal axes, the vortex structure is much more complicated, because the direction of $\mathbf{b}(\boldsymbol{\rho})$ is not a constant.[16,18]

IV. DETERMINATION OF THE UPPER CRITICAL FIELD OF A $YBa_2Cu_3O_{7-\delta}$ SINGLE CRYSTAL FROM REVERSIBLE MAGNETIZATION MEASUREMENTS

In this section we apply the theoretical results of the last two sections to analyze the experimental reversible-magnetization measurements for a $YBa_2Cu_3O_7$ single crystal and obtain the temperature dependence of the upper critical field H_{c2} near the transition temperature T_c. $H_{c2}(T)$ is an important quantity, since it provides information about the microscopic properties of the superconducting state, including the magnitude of the coherence length and the degree of anisotropy.

A twinned single crystal of $YBa_2Cu_3O_7$ was grown by methods described elsewhere.[21] It weighed almost 1 mg and was 110 μm thick. Low-field Meissner measurements showed over 90% flux expulsion, indicating it was close to fully superconducting (see Fig. 6 of Ref. 22). The ac susceptibility[23] showed a single loss peak less than 0.2 K wide, comparable to the best of our samples. The temperature-dependent dc magnetization was measured in a Quantum Design superconducting quantum interference device (SQUID) magnetometer in fields up to 5 T. A scan length of 5 cm was used and the temperature was stabilized to within ± 0.05 K of the target temperature prior to measurement. A 15-min delay was introduced after field changes in order to permit full stabilization of the system. An accuracy of 2×10^{-6} emu was obtained for these measurements. The onset of irreversibility could be detected by a deviation from approximately linear $M(T)$ behavior at lower temperatures.

Figure 2 shows the temperature dependence of the zero-field-cooled magnetization near T_c for various values of applied magnetic field H_a oriented parallel to the c axis (perpendicular to the CuO_2 planes). We observe that the magnetization is reversible in a temperature range of approximately 8 K below T_c. The solid lines are the corresponding theoretical fittings based on the data in the reversible region. The deviation of the experimental points for 1 T from the theoretical curve below 84 K, for example, is attributed to magnetic irreversibility of the sample in this region; the theoretical curve describes only the reversible magnetization.

The fitting procedure is as follows. In the last two sections we obtained a function $-4\pi M'(\tilde{\kappa}, B')$. Note that $B' = H' + 4\pi M'$ gives the connection between the experi-

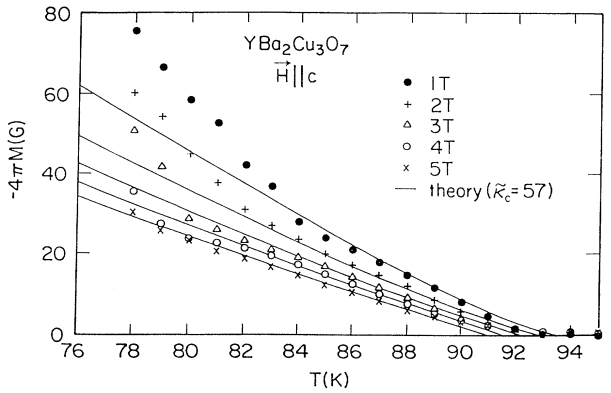

FIG. 2. Magnetization vs temperature for various values of applied fields parallel to the c axis. Points represent data on a 1-mg $YBa_2Cu_3O_7$ crystal, taken in increasing temperature after zero-field cooling; solid curves represent theory described in the text. The deviations of the experimental data from the theoretical curves below about 85 K are due to pinning effects.

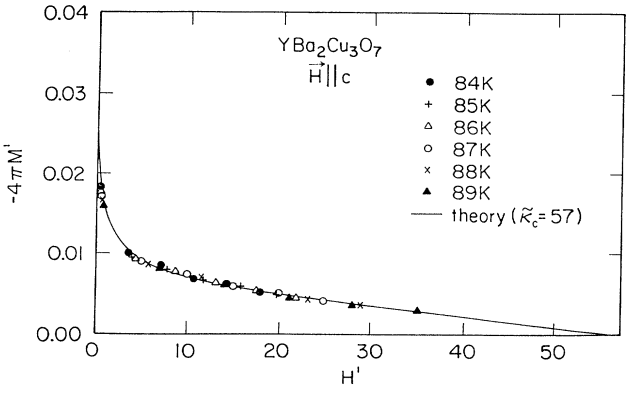

FIG. 3. Magnetization vs applied field in reduced (dimensionless) units. Points represent the same data as in Fig. 2 for a $YBa_2Cu_3O_7$ crystal with field parallel to the c axis. The scaling factor $\sqrt{2}H_c(T)$ and the value of $\tilde{\kappa}_c$ are obtained using the method described in the text.

mental quantities. Here we use primes to denote dimensionless units in which fields are measured in units of $\sqrt{2}H_c(T)$. Because the magnitude of the magnetization is small compared with the applied field, the demagnetization effect can be neglected; thus $H'=H'_a=H_a/\sqrt{2}H_c(T)$. We choose a set of data $\{-4\pi M_i, H_{ai}\}$ $(i=1,2,\ldots)$ at the same T from the reversible region in Fig. 2, and take the ratio $-4\pi M_i/H_{ai}=-4\pi M'/H'$. Assuming a value of $\tilde{\kappa}$, this ratio corresponds to a value of B'. We solve for this value of B', compute the corresponding $-4\pi M'$ and H', and then compute $\sqrt{2}H_c(T)$. We do this for $i=1,2,\ldots$. If the value of $\tilde{\kappa}$ is "right," we get the same value of $\sqrt{2}H_c(T)$ for each data point. The value of $\tilde{\kappa}$ is determined to give the smallest deviation. We then take the average of $\sqrt{2}H_c(T)$ for the chosen $\tilde{\kappa}$. Therefore, from the fitting we obtain both the value of $\tilde{\kappa}$ and the temperature dependence of $H_c(T)$ [or $H_{c2}(T)=\tilde{\kappa}\sqrt{2}H_c(T)$].

The data points used for the fits to obtain $\tilde{\kappa}_c$ and $H_c(T)$ are in the ranges $84\le T\le 89$ K and $1\le H_a\le 5$ T. Here $\tilde{\kappa}_c$ means the value of $\tilde{\kappa}$ for **H** parallel to the c axis. Our best fit gives $\tilde{\kappa}_c=57\pm5$. Figure 3 shows $-4\pi M'$ versus H' of the experimental measurements and the theoretical fitting. Here the range of the error estimate has the meaning that for all values of $\tilde{\kappa}_c$ within the range, the resulting fittings can be considered as good (the differences between any two of them is not obvious to the eye), while for the values of $\tilde{\kappa}_c$ outside the range the resulting fittings clearly become worse than the best one (the differences becomes visually appreciable). In Fig. 4 the solid points exhibit $\sqrt{2}H_c(T)$ versus T, and the line shows a fit to the BCS temperature dependence of $H_c(T)$,[24]

$$\frac{H_c}{H_c(0)}=1.7367\left[1-\frac{T}{T_c}\right]\left[1-0.2730\left[1-\frac{T}{T_c}\right]-0.0949\left[1-\frac{T}{T_c}\right]^2\right], \tag{40}$$

which yields $\sqrt{2}H_c(0)=(1.56\pm0.09)\times10^4$ Oe with $T_c=(94.1\pm10.2)$ K. [If a $1-(T/T_c)^2$ temperature dependence is assumed, slightly lower values of $\sqrt{2}H_c(0)=1.40\times10^4$ Oe and $T_c=93.9$ K are obtained.] The slope $dH_{c2}(T)/dT$ from the fit to the BCS temperature dependence is (-1.65 ± 0.23) T/K at T_c.

To estimate the coherence length at zero temperature one may use the expression $H_{c2\|c}(0)=\phi_0/2\pi\xi^2_{ab}(0)$, where we ignore anisotropy in the ab plane. The relationship between $H_{c2}(0)$ and dH_{c2}/dT at T_c in the isotropic superconductors is[4,25]

$$H_{c2}(0)=0.5758\left[\frac{\kappa_1(0)}{\kappa}\right]T_c\left|\frac{dH_{c2}}{dT}\right|_{T_c}. \tag{41}$$

In the dirty limit $\kappa_1(0)/\kappa=1.20$,[26,27] while in the clean limit $\kappa_1(0)/\kappa=1.26$.[28] These expressions yield $\xi_{ab}(0)=(17.6\pm1.3)$ Å assuming the dirty limit and $\xi_{ab}(0)=(17.2\pm1.2)$ Å assuming the clean limit.

As discussed in the Introduction, evidence favors the clean limit. The deduced $H_{c1\|c}(0)$ and $H_{c2\|c}(0)$ are (784 ± 12) Oe and (112 ± 16) T, respectively. The $H_{c1\|c}(0)$ value agrees reasonably with extrapolated values from high-temperature flux penetration experiments,[29] though not with low-temperature studies which give much higher values,[30–32] but which may be affected by surface barriers. The $H_{c2\|c}(0)$ values are significantly larger than values reported in pulsed field measurements,[33] which may indicate some problem in the extrapolation to low

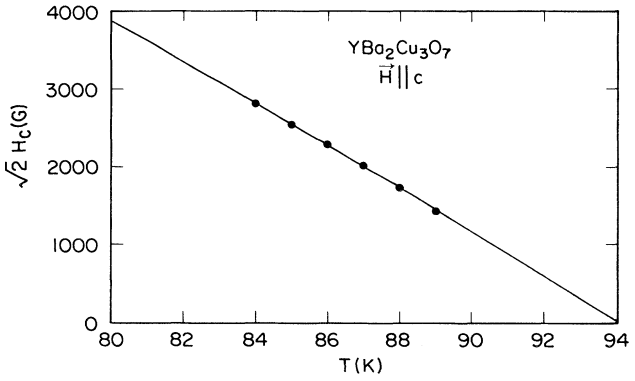

FIG. 4. The temperature dependence of $\sqrt{2}H_c$ (points) and the fit to the BCS temperature dependence (solid curve), deduced from magnetization data on a $YBa_2Cu_3O_7$ crystal with field parallel to the c axis.

temperature. The thermodynamic critical field $H_c(0)$ is (1.10±0.06) T.

The theoretical curves of $-4\pi M$ versus T in Fig. 2 are calculated using the above fitting results. The slope of $-4\pi M(T)$ for constant H_a is given by

$$\frac{\partial(-4\pi M)}{\partial T}=\left[H'\frac{dB'}{dH'}-B'\right]\frac{d(\sqrt{2}H_c)}{dT}\ , \tag{42}$$

which becomes H_a independent in the Abrikosov linear region,

$$\frac{\partial(-4\pi M)}{\partial T}=\frac{1}{(2\tilde{\kappa}^2-1)\beta_A}\frac{dH_{c2}}{dT}\quad(\beta_A=1.16)\ . \tag{43}$$

As we can see from the solid curves in Fig. 2, the Abrikosov linear region (as calculated from the mean-field theory neglecting fluctuations) is limited to values of T *very* close to T_c for these values of H_a. For example, for $H_a=1$ T this region is restricted to a region of the reduced temperature $(T_{c2}-T)/T_c<0.02$. The field dependence of the slope shows that the apparently linear curves in the lower-temperature region are outside the true Abrikosov linear region. Figure 3 shows more clearly that the majority of the data points are in the lower-field region where Abrikosov's high-field result does not apply. Therefore, the conventional procedure in which one focuses on the apparently linear region at the lower temperatures and extrapolates to $-4\pi M=0$, ignoring the region near T_c, results in values for T_{c2} and T_c that are too small and a magnitude of the slope of H_{c2} versus T that is too large. The reason that the slope of $H_{c2}(T)$ is less with the present method of analysis is that the difference between T_{c2} by the present method and T_{c2} by the conventional method is greater at lower fields than at higher fields.

We also find that in order to fit the data in the region $T\geq 90$ K, much larger and temperature-dependent values of $\tilde{\kappa}_c$ must be used, e.g., $\tilde{\kappa}_c=70$ for $T=90$ K and $\tilde{\kappa}_c=110$ for $T=91$ K. Such behavior is very different from the prediction of the Ginzburg-Landau mean-field theory, according to which the value of $\tilde{\kappa}_c$ is a constant near T_c. This suggests that $T\geq 90$ K is a fluctuation region where the mean-field theory becomes invalid.

The extrapolated transition temperature of (94.1±0.2) K can be compared to the observed onset of ac loss in the 1-MHz ac susceptibility at (93.7±0.1) K and a loss peak at (93.5±0.1) K. While these values are just about within experimental error of each other, the results suggest that the diamagnetic mean-field T_c may be slightly higher than the true T_c, as expected theoretically.[8] However, such shifts due to critical phenomena are clearly small, limited to a few tenths of a degree at most.

In summary, we have introduced a new method for obtaining from the Ginzburg-Landau theory a good approximate analytic expression for the mean-field-theory magnetization of an anisotropic superconductor as a function of field H for all values in the range H_{c1} to H_{c2}. We have applied this method to analyze experimental magnetization data from a single crystal of $YBa_2Cu_3O_7$, taken as a function of temperature at constant values of the applied magnetic field. We have obtained a good determination of the upper critical-field slope for H parallel to the c axis by making use of the data in a window of temperatures above those for which flux pinning makes the magnetization curves irreversible and below those near T_c where fluctuations occur.

ACKNOWLEDGMENTS

The authors acknowledge useful conversations with T. K. Worthington, M. Daeumling, L. Krusin-Elbaum, G. Crabtree, U. Welp, and V. G. Kogan. Ames Laboratory is operated for the U.S. Department of Energy by Iowa State University under Contract No. W-7405-Eng-82. This work was supported by the Director for Energy Research, Office of Basic Energy Sciences. It also was supported in part by IBM and the Oak Ridge National Laboratory High Temperature Superconductivity Program, Office of Energy Storage and Distribution, Conservation and Renewable Energy, under Contract No. DE·AC05-84OR21400, with Martin Marietta Energy Systems, Inc.

APPENDIX A: CALCULATION OF THE LOCAL MAGNETIC FLUX DENSITY

For a two-dimensional array of vortices at the positions $\boldsymbol{\rho}_i=\mathbf{L}$, where $\mathbf{L}$ is a lattice vector, there is a corresponding two-dimensional reciprocal lattice of lattice vector $\mathbf{G}$ such that $e^{i\mathbf{G}\cdot\mathbf{L}}=1$. Now let us introduce the Fourier transform of b_{0z} given by Eq. (13)

$$\tilde{b}_{0z}(q)=\int d^2\rho\, b_{0z}(\rho)e^{-i\mathbf{q}\cdot\boldsymbol{\rho}}$$
$$=\frac{2\pi f_\infty K_1(\xi_v(q^2+f_\infty^2)^{1/2})}{\kappa(q^2+f_\infty^2)^{1/2}K_1(f_\infty\xi_v)}\ , \tag{A1}$$

where we have used the formulas[34,35]

$$\frac{1}{\pi}\int_0^\pi d\theta\, e^{ix\cos\theta}=J_0(x) \tag{A2}$$

and

$$\int_0^\infty dx\, xJ_0(\beta x)K_0(\alpha(x^2+z^2)^{1/2}) = \frac{zK_1(z(\alpha^2+\beta^2)^{1/2})}{(\alpha^2+\beta^2)^{1/2}} . \quad \text{(A3)}$$

(Note that $\tilde{b}_{0z}(0)=2\pi/\kappa$ is the flux quantum.) Then Eq. (11) becomes

$$\begin{aligned} b_z(\boldsymbol{\rho}) &= \sum_{\mathbf{L}} b_{0z}(\boldsymbol{\rho}-\mathbf{L}) \\ &= \sum_{\mathbf{L}} \int \frac{d^2q}{(2\pi)^2} \tilde{b}_{0z}(q) e^{i(\boldsymbol{\rho}-\mathbf{L})\cdot\mathbf{q}} \\ &= \frac{1}{A_{\text{cell}}} \sum_{\mathbf{G}} \tilde{b}_{0z}(G) e^{i\boldsymbol{\rho}\cdot\mathbf{G}} , \end{aligned} \quad \text{(A4)}$$

where the relation

$$A_{\text{cell}} \sum_{\mathbf{L}} e^{i\mathbf{L}\cdot\mathbf{q}} = (2\pi)^2 \sum_{\mathbf{G}} \delta(\mathbf{q}-\mathbf{G}) \quad \text{(A5)}$$

has been used. Using the fact that $B=2\pi/\kappa A_{\text{cell}}$ and separating the term with $\mathbf{G}=\mathbf{0}$ from the summation, the above equation becomes

$$b_z(\boldsymbol{\rho}) = B\left[1+\sum_{\mathbf{G}\neq\mathbf{0}} \frac{f_\infty K_1(\xi_v(G^2+f_\infty^2)^{1/2})}{(G^2+f_\infty^2)^{1/2}K_1(f_\infty\xi_v)} e^{i\boldsymbol{\rho}\cdot\mathbf{G}}\right] . \quad \text{(A6)}$$

The magnetic flux density at the vortex center is obtained by setting $\boldsymbol{\rho}=\mathbf{0}$:

$$b_z(0) = B\left[1+\sum_{\mathbf{G}\neq\mathbf{0}} \frac{f_\infty K_1(\xi_v(G^2+f_\infty^2)^{1/2})}{(G^2+f_\infty^2)^{1/2}K_1(f_\infty\xi_v)}\right] . \quad \text{(A7)}$$

We approximate the summation in $\mathbf{G}$ space by an integral taken over the outside of the first Brillouin zone:

$$\sum_{\mathbf{G}\neq\mathbf{0}} \approx \frac{1}{A_{\text{BZ}}} \int_{G\geq G_{\text{BZ}}} d^2G , \quad \text{(A8)}$$

where $A_{\text{BZ}}=\pi G_{\text{BZ}}^2=(2\pi)^2/A_{\text{cell}}$ is the area of the first Brillouin zone, and the zone boundary has been approximated by a circle of radius G_{BZ}. That $B=2\pi/\kappa A_{\text{cell}}$ gives $G_{\text{BZ}}=\sqrt{2B\kappa}$. Note that, although the approximation of Eq. (A8) is valid only at low field when the reciprocal lattice spacing (which is inversely proportional to the vortex spacing) is small, for high field the error due to the approximation is reduced by the fact that the contribution of the sum becomes small compared to that of the $\mathbf{G}=\mathbf{0}$ term; we therefore use the approximation for the whole field region. Thus, we get

$$b_z(0) = B + \frac{f_\infty K_0(\xi_v(f_\infty^2+2B\kappa)^{1/2})}{\kappa\xi_v K_1(f_\infty\xi_v)} . \quad \text{(A9)}$$

The above equation shows the properties that $b_z(0)\to b_{0z}(0)$ when $B\to 0$ and $b_z(0)\to B$ when B becomes large.

[1] A. A. Abrikosov, Zh. Eksp. Teor. Fiz. **32**, 1442 (1957).

[2] V. L. Ginzburg and L. D. Landau, Zh. Eksp. Teor. Fiz. **20**, 1064 (1950) [English trans. in *Men of Physics: L. D. Landau,* edited by D. ter Haar (Pergamon, New York, 1965), Vol. 1 pp. 138-167].

[3] P. G. de Gennes, *Superconductivity of Metals and Alloys,* (Benjamin, New York, 1966).

[4] A. L. Fetter and P. C. Hohenberg, in *Superconductivity,* edited by R. D. Parks (Marcel Dekker, New York, 1969), p. 817.

[5] J. R. Clem, J. Low Temp. Phys. **18**, 427 (1975).

[6] J. R. Clem, in *Low Temperature Physics–LT14,* edited by M. Krusius and M. Vuorio (North-Holland, Amsterdam, 1975), Vol. 2, pp. 285-288.

[7] A. P. Malozemoff, in *Physical Properties of High Temperature Superconductors,* edited by D. Ginsberg (World Scientific, Singapore, 1989), p. 71.

[8] D. Fisher, M. P. A. Fisher, and D. A. Huse, Phys. Rev. B **43**, 130 (1991).

[9] U. Welp, W. K. Kwok, G. W. Crabtree, K. G. Vandervoort, and J. Z. Liu, Phys. Rev. Lett. **62**, 1908 (1989).

[10] T. Penney, S. von Molnar, D. Kaiser, F. Holtzberg, and A. W. Kleinsasser, Phys. Rev. B **38**, 2918 (1988); T. K. Worthington, F. Holtzberg, and C. Feild, Cryogenics **30**, 417 (1990); values of 65 $\mu\Omega$ cm for ρ_{ab}(100 K) have also been measured by N. C. Yeh and F. Holtzberg (unpublished) on several more recent crystals from the batches which produced the crystal used in the present study.

[11] E. Osquiguil, R. Decca, G. Nieva, L. Civale, and F. de la Cruz, Solid State Commun. **65**, 491 (1987).

[12] N. E. Bickers, D. J. Scalapino, R. T. Collins, and Z. Schlesinger, Phys. Rev. B **42**, 67 (1990).

[13] J. R. Clem, in *Superconducting Electronics,* edited by H. Weinstock and M. Nisenoff (Spring-Verlag, Berlin, 1989), p. 1.

[14] V. L. Ginzburg, Zh. Eksp. Teor. Fiz. **23**, 326 (1952).

[15] D. R. Tilley, Proc. Phys. Soc. London **85**, 1177 (1965).

[16] K. Takanaka, Phys. Status Solidi B **68**, 623 (1975).

[17] R. A. Klemm and J. R. Clem, Phys. Rev. B **21**, 1868 (1980).

[18] V. G. Kogan, Phys. Rev. B **24**, 1572 (1981).

[19] V. G. Kogan and J. R. Clem, Phys. Rev. B **24**, 2497 (1981).

[20] R. A. Klemm, Phys. Rev. B **38**, 6641 (1988).

[21] D. L. Kaiser, F. Holtzberg, B. A. Scott, and T. R. McGuire, Appl. Phys. Lett. **51**, 1040 (1987).

[22] L. Krusin-Elbaum, A. P. Malozemoff, D. C. Cronemeyer, F. Holtzberg, J. R. Clem, and Z. Hao, J. Appl. Phys. **67**, 4670 (1990).

[23] T. K. Worthington, W. J. Gallagher, D. L. Kaiser, F. Holtzberg, and R. L. Sandstrom, Physica B **148**, 228 (1987).

[24] J. R. Clem, Ann. Phys. (N.Y.) **40**, 268 (1966).

[25] B. Mühlschlegel, Z. Phys. **155**, 313 (1959).

[26] N. R. Werthamer, E. Helfand, and P. C. Hohenberg, Phys. Rev. **147**, 295 (1966).

[27] K. Maki, Phys. Rev. **148**, 362 (1966).

[28] G. Eilenberger, Phys. Rev. **153**, 584 (1967).

[29] L. Krusin-Elbaum, A. P. Malozemoff, Y. Yeshurun, D. C. Cronemeyer, and F. Holtzberg, Phys. Rev. B **39**, 2936 (1989).

[30] V. V. Moshcholkov, O. V. Petrenko, A. A. Zhukov, A. A. Gippins, V. I. Voronkova, V. S. Belov, and V. A. Rybachuk, Physica C **162-164**, 1611 (1989).

[31]A. Umezawa, G. W. Crabtree, K. G. Vandervoort, U. Welp, W. K. Kwok, and J. Z. Liu, Physica C **162-164**, 733 (1989).
[32]M. W. McElfresh, Y. Yeshurun, A. P. Malozemoff, and F. Holtzberg, Physica A **168**, 308 (1990).
[33]T. Sakakibara, T. Goto, and N. Miura, Technical Report of ISSP, University of Tokyo, Ser. A, No. 1976, 1988 (unpublished).
[34]*Handbook of Mathematical Functions* edited by M. Abramowitz and I. A. Stegun (National Bureau of Standards, Washington, DC, 1964), p. 360.
[35]I. S. Gradshteyn and I. M. Ryzhik, *Tables of Integrals, Series, and Products* (Academic, New York, 1965), p. 706.